Uncovering the Neural Mechanisms of Inter-Hemispheric Balance Restoration in Chronic Stroke Through EMG-Driven Robot Hand Training: Insights From Dynamic Causal Modeling

Chun-Hang Eden Ti, Chengpeng Hu, Kai Yuan, Winnie Chiu-Wing Chu, and Raymond Kai-Yu Tong, *Senior Member, IEEE*

***Abstract*— EMG-driven robot hand training can facilitate motor recovery in chronic stroke patients by restoring the interhemispheric balance between motor networks. However, the underlying mechanisms of reorganization between interhemispheric regions remain unclear. This study investigated the effective connectivity (EC) between the ventral premotor cortex (PMv), supplementary motor area (SMA), and primary motor cortex (M1) using Dynamic Causal Modeling (DCM) during motor tasks with the paretic hand. Nineteen chronic stroke subjects underwent 20 sessions of EMG-driven robot hand training, and their Action Reach Arm Test (ARAT) showed significant improvement (β=3.56, p<0.001). The improvement was correlated with the reduction of inhibitory coupling from the contralesional M1 to the ipsilesional M1 (r=0.58, p=0.014). An increase in the laterality index was only observed in homotopic M1, but not in the premotor area. Additionally, we identified an increase in resting-state functional connectivity (FC) between bilateral M1 (β=0.11, p=0.01). Inter-M1 FC demonstrated marginal positive relationships with ARAT scores (r=0.402, p=0.110), but its changes did not correlate with ARAT improvements. These findings suggest that the improvement of hand functions brought about by EMG-driven robot hand training was driven explicitly by task-specific reorganization of motor networks. Particularly, the restoration of interhemispheric balance was induced by a reduction in interhemispheric inhibition from the contralesional M1 during motor tasks of the paretic hand. This finding sheds light on the mechanistic understanding of interhemispheric balance and functional recovery induced by EMG-driven robot training.**

***Index Terms*— Dynamic causal modeling, effective connectivity, resting-state functional connectivity, interhemispheric, chronic stroke.**

Nomenclature

ARAT	The Action Reach Arm Test.
cM1	Contralesional primary motor cortex.
cPMv	Contralesional ventral premotor area.
cSMA	Contralesional supplementary motor area.
DCM	Dynamic Causal Modelling.
FMA-UE	The Fugl-Meyer Assessment for upper extremity.
iM1	Ipsilesional primary motor cortex.
iPMv	Ipsilesional ventral premotor area.
iSMA	Ipsilesional supplementary motor area.

I. Introduction

STROKE is a prevalent cause of disability, with a majority of stroke survivors suffering from upper limb paresis [1]. The consequences of upper limb extremity impairment persist for over six months, and only a small proportion of stroke survivors (less than 12%) can achieve full functional recovery [2]. Research has been dedicated to developing post-stroke motor rehabilitation protocols to restore the upper limb functions in order to restore their Activities of Daily Living (ADL) and enhance their quality of life.

A growing interest in robot-assisted devices for upper limb rehabilitation has been seen in recent decades [3]. Robotic rehabilitation offers a consistent, intensive, and interactive training experience that engages individuals [4]. Recent meta-analysis demonstrated that individuals who underwent training with robot-assisted devices improved better in Fugl-Meyers Assessment scores on Upper Extremity (FMA-UE) and functional activity [5], [6]. However, wrist and hand robots have

Manuscript received 12 April 2023; revised 23 October 2023 and 29 November 2023; accepted 2 December 2023. Date of publication 5 December 2023; date of current version 12 January 2024. This work was supported in part by the General Research Fund under Grant 14205419; and in part by the Research Grant Council of Hong Kong, Hong Kong. *(Chun-Hang Eden Ti and Chengpeng Hu contributed equally to this work.) (Corresponding author: Raymond Kai-Yu Tong.)*

This work involved human subjects or animals in its research. Approval of all ethical and experimental procedures and protocols was granted by the Joint Chinese University of Hong Kong-New Territories East Cluster Clinical Research Ethics Committee under Reference No. 2018.661.

Chun-Hang Eden Ti, Chengpeng Hu, Kai Yuan, and Raymond Kai-Yu Tong are with the Department of Biomedical Engineering, The Chinese University of Hong Kong, Hong Kong (e-mail: kytong@cuhk.edu.hk).

Winnie Chiu-Wing Chu is with the Department of Imaging and Interventional Radiology, The Chinese University of Hong Kong, Hong Kong.

This article has supplementary downloadable material available at https://doi.org/10.1109/TNSRE.2023.3339756, provided by the authors.

Digital Object Identifier 10.1109/TNSRE.2023.3339756

limited effects on motor control and improvement of ADL [7]. In the past five years, intention-driven robots have become popular in improving wrist and hand functions in motor rehabilitation [8], [9], [10]. By utilizing electrophysiological signals such as Electroencephalogram (EEG) or electromyography(EMG), individuals can actively trigger robot-assisted motor tasks by initiating voluntary movement intentions [11]. Clinical studies have found that training with EMG-driven robot hands resulted in better FMA-UE scores, improved wrist and hand functions assessed by Action Reach Arm Test(ARAT), and enhanced muscle coordination on wrist and elbow joints compared to the control group receiving continuous passive movements [12], [13]. The effect of this recovery persisted for more than 6 months, suggesting a lasting change in brain activity due to the robot hand training. Indeed, active engagement in voluntary motor intention has been shown to induce neural plasticity in motor learning [14]. However, The precise neurophysiological mechanisms of the motor recovery induced by these devices are still limited.

Maladaptive plasticity often emerges during stroke recovery, leading to a hyperreliance on contralesional activity when patients perform motor tasks with the paretic hand.Compensatory movement patterns that rely on the trunks and proximal side of the paretic hand, and the disuse of paretic hand, contribute to strengthened contralesional motor projections [15], [16]. Persistent contralesional cortical activity after 6-12 months of stroke usually leads to poor motor recovery due to excessive interhemispheric inhibition on the ipsilesional motor area [17], [18]. Furthermore, increased activation of the contralesional motor area contributes to abnormal interjoint coupling after stroke, impairing the execution of reaching and grasping movements [19]. EMG-driven hand robots overcome maladaptive plasticity by encouraging voluntary hand opening and grasping that enhance the reorganization of internal sensorimotor representation through Hebbian learning, and restore interhemispheric balance [20].

A recent systematic review has indicated that intention-driven robot hand promotes motor recovery through the remodeling of interhemispheric interactions [21]. Particularly, studies have identified an ipsilesional shift in activation and corticomuscular integration during tasks with paretic hand [22], [23]. Studies using Transcranial Magnetic Stimulation(TMS) identified increased ipsilesional corticospinal excitability to the target muscles [24]. These studies demonstrated that motor recovery involved network reorganization that re-establishes a normalized interhemispheric balance. Nevertheless, the role and interplay of brain regions involved in motor recovery are not well understood. Secondary motor regions, including the dorsal premotor cortex (PMd), ventral premotor cortex(PMv) and supplementary motor area(SMA) are actively involved during the recovery process [25]. Secondary motor regions were considered substitutes for M1 for cortical projection and executive motor functions [26]. These regions also work together to generate desired motor responses. For instance, the SMA is mainly responsible for planning and coordination of motor tasks [27], [28]. PMd and PMv are involved in movement initiation and generating mental representation of motor responses [29], [30]. The integration between these brain regions, and its implications on motor recovery requires more investigation.

Dynamic Causal Modeling (DCM) is a framework that provides insights into dynamic interactions between different brain regions. Effective connectivity(EC) measured from DCM characterizes the excitatory or inhibitory coupling within the defined motor systems. Grefkes and his colleagues have applied DCM analysis to investigate brain network interactions in stroke survivors in a series of studies [31], [32], [33]. These studies provide compelling evidence that inter-hemispheric inhibition between the primary motor cortex (M1) is a crucial pathophysiological factor in motor impairment at all stages of stroke and is also a biomarker for motor recovery [31], [32]. Additionally, the coupling from ipsilesional premotor to motor regions also demonstrated supportive role in motor recovery in chronic stroke [32]. Analyzing the EC between motor systems before and after EMG-driven robot hand training enables a better understanding on the causal nature of these functional interactions, and their associations with upper extremity improvements. In particular, a recent Parametric Empirical Bayes (PEB) framework had been introduced to discern network reorganization patterns due to training [34]. The approach performed second-level Bayesian Model Reduction to identify the optimal network interactions that explain the change in network activity due to the training, hence providing better understanding on the underlying mechanisms of robot-mediated learning.

Apart from effective connectivity, resting-state functional connectivity (FC) is widely used to study the motor network interactions in stroke. FC measures the spatial-temporal correlation of spontaneous brain activity between regions during resting-state fMRI acquisition [35], [36]. Studies of FC within motor networks in stroke have provided insights regarding motor impairment and functional reorganization during motor recovery [37], [38]. For instance, Cartel et al. reported that disruption of inter-hemispheric FC between homologous M1 and premotor regions predicts the motor deficits in sub-acute stroke [39], and interhemispheric FC between M1 positively correlates with functional recovery [40]. Resting-state FC and task-modulated EC distinctive information on brain network reorganization associated with individuals impairment and state of motor recovery [41]. Paul et al. has reported that EC captures state-dependent causal interactions while FC reflects state-independent mechanisms of network reorganization [41]. Analyzing EC and FC together therefore enables a better understanding of neural plasticity mediated by EMG-driven robots, of whether network reogranization happens as a general change in brain interactions or specific change induced by a motor task.

Limited research has been conducted to examine the effects of EMG-driven robot training on the directed causal influence between motor regions. A recent study on directed corticomuscular coupling in stroke identified distinct associations between promixal-to-distal compensatory movement and the alteration of descending motor pathways and ascending feedback [42]. The study demonstrated that the direction of information flow between coupled regions provides additional insights into cortical interactions beyond mere synchrony.

TABLE I
DEMOGRAPHIC INFORMATION OF THE INCLUDED SUBJECTS IN THIS STUDY

Variables	N = 17†	
Numerical variables	Mean(SD)	Median(SD)
Age(yrs)	60.7(9.91)	62(16.5)
TSS(yrs)	4.29(3.57)	3(3.25)
pre-ARAT	29.7(13.6)	34(25)
Categorical variables		
Gender	7M 10F	
Stroke Type	13I 4H	
Affected hand	9D 9ND	

† One subject withdrew the study and one subject was excluded from the fMRI analysis due to improper identification of ipsilesional ROIs. The detailed demographic information of each individual is listed in the Supplementary Tables S2. Abbreviations: D=Dominant hand; H=Haemorrhagic stroke; I=Ischemic stroke; ND=Non-dominant hand; TSS=Time since stroke;

Similarly, the information flow between motor network in responses to EMG-driven robot hand training has yet to be studied. Our study is the first to analyze the reorganization of effective connectivity between motor networks induced by EMG-driven robot hand training using Dynamic Causal Modeling. We conducted a study on 19 chronic stroke survivors who underwent 20 sessions of EMG-driven robot hand training. Using Parametric Empirical Bayes approach, we identified the connectome that best explains the average effective connectivity and the training-induced change during motor tasks of paretic hand. We also studied the FC of the corresponding region pairs to examined the task-independent cortical reorganization process, and their associations with motor improvement. Lastly, We computed the weighted laterality index (wLI) of activation during motor tasks to assess changes in inter-hemispheric balance of motor activation. This study sheds new light on the mechanistic understanding of interhemispheric balance contributing to the functional recovery in chronic stroke subjects brought about by EMG-driven robot hand training.

II. MATERIALS AND METHODS

A. Participant

We conducted a monocenter, randomized controlled trial, in which participants were randomized into personalized tDCS-combined robot hand training (Stimulation group) or Sham tDCS-combined robot hand training (Sham group). This study was approved by the Joint Chinese University of Hong Kong New Territories East Cluster Clinical Research Ethics Committee, and the clinical trial was registered with ClinicalTrials.gov (NCT05638464). Nineteen chronic stroke survivors were recruited for this study. One subject withdrew the study due to medical reason, and one subject was excluded from the fMRI analysis due to abnormal fMRI activation pattern. A brief summary of their demographical information is presented in Table I and the details are presented in Supplementary Table II.1. All subjects signed a written consent confirming that they understood the procedures and implications of the study. The subjects met the following inclusion criteria: (1) First-ever stroke, (2) Six months after onset of stroke, (3) Unilateral brain lesions, (4) Moderate to severe upper limb dysfunctions assessed by the Action Research Arm Test (ARAT), with scores between 6-52. Subjects with (1) a family history of epilepsy, (2) alcohol or drug abuse, (3)neurological dysfunctions such as spatial neglect, aphasia, apraxia, (4) cortical lesions located on the primary motor cortex, (5) or other dysfunctions that prevented subjects from understanding instructions were excluded from our study. ARAT was used to assess motor functions of stroke subjects before (*Pre*) and after (*Post*) training sessions.

B. Training Intervention Protocols

Each subject completed 20 sessions of tDCS-combined EMG-driven robot hand training at the local community center. The robotic hand design and training details were previously reported in our study [43]. Before training commenced, each subject underwent 20 minutes of active or sham tDCS depending on the allocated group. The details of the stimulation procedure is presented in Supplementary Methods S1.3. Stimulation lasted for 20 minutes prior to training. During training, subjects wore the robotic hand and were seated comfortably facing a computer screen. They were instructed to keep their elbow at rest and slightly flexed at approximately 130°. EMG signals were recorded from the Flexor Digitorum (FD) and Extensor Digitorum (ED) muscles, with reference electrodes placed over the olecranon process of the paretic arm (as shown in Figure 1a). To measure voluntary motor intention, subjects were instructed to perform maximum voluntary contraction (MVC) with the robotic hand fixated at its fully-extended and fully-flexed position. MVC for FD and ED were then collected by performing maximal isometric contraction by grasping or opening their hand with all digits at maximal force respectively. The training consisted of 3 task blocks, each lasting 15 minutes with an interleaved 5-minute break. Within each block, subjects were required to trigger the robot-assisted grasping and opening by producing EMG signal of the corresponding muscle exceeding 10% of the MVC signal according to the practice in our previous study [43]. Trials were repeated until the end of each block. Successful trigger times are defined as the sum of the number of trials completed by the subject in all three blocks. During the trials, an experienced physical therapist observed the signs of involuntary spastic muscle contraction by monitoring the real-time EMG amplitudes, and adjusted the MVC threshold upwards, up to 50% MVC accordingly, to reduce the likelihood of trigger robot-assisted movement with involuntary motor intention. Figure 1(a) shows the set-up for the robot-hand training.

C. MRI Data Acquisition

MRI scans were recorded using a 20-channel head coil by MAGNETOM PRISMA 3.0T XR Numaris(SIEMENS, Munich, Germany) for all 19 subjects. High-resolution anatomical T1 images were acquired using T1-MPRAGE sequence (TR/TE = 1900/2.93 ms, flip angle = 9°, 176 slices, voxel size = $0.9 \times 0.9 \times 1.0\ mm^3$). Resting-state (rs-fMRI) and task-based fMRI (tb-fMRI) data were acquired in BOLD images using EPI-FID sequences (TR/TE = 1200/30 ms, flip angle = 68°, 48 slices, voxel size = $3.0 \times 3.0 \times 3.0\ mm^3$).

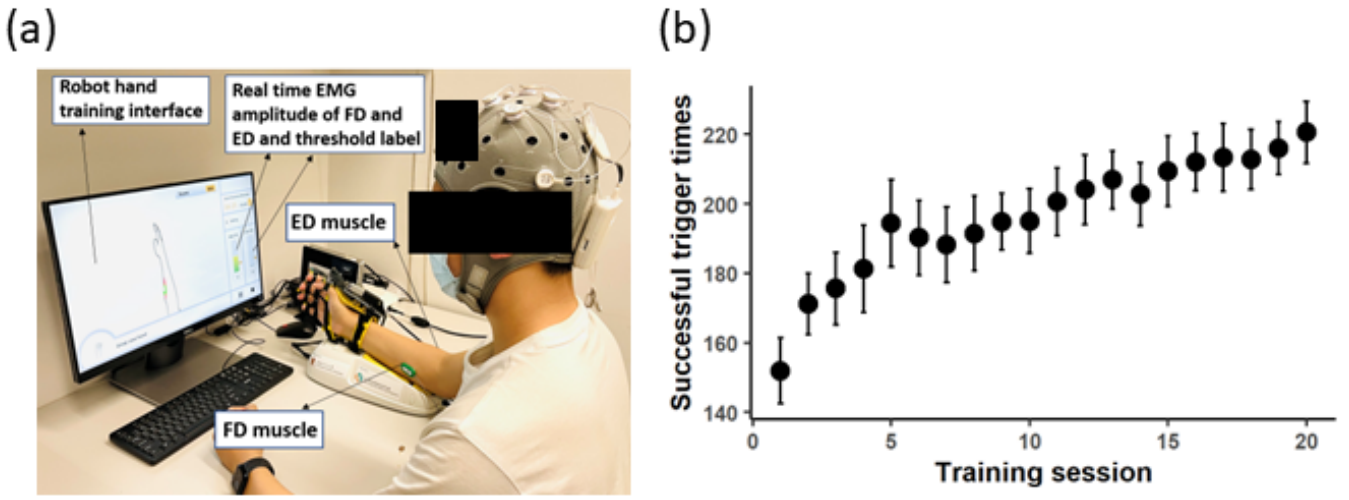

Fig. 1. (a) Setup for the EMG-driven robot hand training. (b) Average training progress of the participants included in this study. Average number of successful triggers in each session is represented in black dots. Error bar demotes 1 standard error from the mean.

Each subject completed two MRI sessions, before (*Pre*) and immediately after(*Post*) 20 sessions of robot-hand training, during which both tb-fMRI and rs-fMRI were acquired. During task fMRI, the subject was required to grasp a tennis unimanually, with either the left or right hand, according to the text cue displayed on the screen. Each trial lasted for 6 seconds followed by a 14.4-second resting period before the start of the next trial. The block consists of 20 trials, with 10 trials for each condition arranged in a randomized order. Afterward, a 6.5-minute resting-state fMRI was acquired while the subject fixated on a white fixation cross at the center of the screen while minimizing thoughts and movements. All instructions and fixations were presented using EPrime3.0 (Psychology Software Tools, PA USA).

D. fMRI Analysis

1) Preprocessing: All fMRI data from subjects with left-hemispheric lesions were flipped along the mid-sagittal plane, resulting in the right hemisphere being designated as the ipsilesional hemisphere. Preprocessing of the rs-fMRI and task-based fMRI data was carried out using the DPARSF function in the DPABI toolbox [44]. Initially, the fMRI volumes of each session of rs-fMRI were realigned with the first volume of the first session. Brain tissues were then segmented from each subject's anatomical T1 images using SPM12 New Segment + DARTEL [45]. For the rs-fMRI data, Friston-24 head motion parameters, as well as the mean signal from white matter and cerebrospinal fluid, were included as nuisance regressors to mitigate motion and physiological-related artifacts. Subsequently, all preprocessed images were bandpass filtered between 0.1 Hz to 1 Hz, normalized to the Montreal Neurological Institute (MNI) standard template, and spatially smoothed with a 6-mm full-width at half maximum (FWHM) Gaussian filter for further analysis.

2) ROI Definition and Extraction of Timeseries for Connectivity Analysis: The motor regions of the brain, including the primary motor cortex (M1), ventral premotor cortex (PMv), and supplementary motor area (SMA), play a key role in hand grasping and are commonly studied in connectivity analysis [41], [46]. To identify individual ROIs, individual tb-fMRI volumes were subjected to first-level General Linear Model (GLM) analysis to estimate the BOLD activation during motor execution of thier paretic hand (IPSI) and non-paretic hand(CONTRA) respectively. The model specification and estimation were included in Supplementary Methods. Contrast maps for each condition over all subjects and sessions were averaged to obtain a group-level activation map. The initial coordinate of each ROI was defined as the peak value of the group-level activation map within an apriori mask using the Automated anatomical labelling atlas [47]. Subsequently, individual ROIs were defined as the local activation maxima within a 15-mm sphere around the initial seed location. This approach ensured that individual activation maxima were identified, thus avoiding the inclusion of non-functional regions due to stroke lesions [41].

To extract the ROI signals, we obtained the first eigenvariate of the timeseries of all voxels within an 8-mm sphere around the local activation maxima. Ipsilesional and contralesional ROIs were determined using IPSI and CONTRA contrasts, respectively. One subject was excluded from the fMRI analysis due to improper identification of ipsilesional ROIs. The seed locations for each ROI of each individual are listed in the Supplementary Table S3.

3) Estimation of Task-Related and Endogenous Effective Connectivity: We used Dynamic Causal Modeling (DCM) to estimate effective connectivity (EC) between brain regions. DCM is a generative model that links observed blood-oxygen-level-dependent (BOLD) responses to the intrinsic neuronal states of a deterministic system of brain activity with specified regions of interest (ROIs). The neuronal state of the system is represented by the variable z, and the rate of change in z is given by Equation 1.

$$\frac{dz}{dt} = [A + \sum_{j=1}^{m} u_j B^{(j)}]z + Cu \tag{1}$$

In this equation, u represents experimental conditions, A, B, and C are matrices representing the coupling parameters

between defined ROIs, with A capturing the average endogenous EC between ROIs across experimental conditions, B representing the task-modulated EC elicited by given experimental conditions, and C representing the direct extrinsic influence of the state with respect to given experimental inputs.

To estimate task-modulated effective connectivity (Matrix B) for each subject and session, DCM with fully connected A and B matrices and driving inputs on bilateral premotor areas was estimated. The training effect was quantified using a Parametric Empirical Bayesian (PEB) approach [34]. The PEB framework assumed an equal network architecture with varying connection strength for each subject, and variability of the coupling parameters was explained by coupling shared between subjects (commonalities) and coupling explained by defined regressors. The main regressor, TIME (+1 for $Post$ and -1 for Pre), and covariate regressors, including individual Gender, Age, Time Since Stroke (TSS), Affected hand, and pre-ARAT scores, were included to quantify the training effect after training. The estimated PEB estimates for the TIME regressor corresponded to the training effect on each coupling parameter of the DCM B Matrix.

To optimize the best model to explain the experimental effect, we performed Bayesian Model Reduction (BMR) to compare the model evidence between fully-connected models with a reduced model, by switching the parameters on or off [48]. To limit the number of model comparisons, we defined 44 sets of candidate models, following the study in [41]. These models were constructed based on the lateralization and directionality of the connectome. A lateralized network only involves with the M1 contralateral to the moving hands, whereas both M1s is invovled in non-lateralized networks. A unidirectiaonl network implies that M1 only receives command from premotor areas, whereas a bidirectional network means M1 both receive and send outputs to the premotor areas. Bayesian Model Average (BMA) was obtained by averaging the PEB parameters weighted by the posterior probabilities of the respective models. Averaged PEB estimates were thresholded to exclude connections with less than a 0.01 probability of being present. Finally, the BMA estimates were used as empirical priors for estimating individual ECs through a first-level reduced DCM model. We performed Pearson correlation between the EC values and ARAT scores at *Pre* and *Post* sessions, and the change of EC (ΔEC) and change of ARAT scores (ΔARAT).

We performed separately analysis for endogenous effective connectivity (Matrix A). Procedures and results were reported in Supplementary Results. All DCM analyses were performed using SPM12 [34], [49].

4) Estimation of Resting-State Functional Connectivity: Functional connectivity (FC) was estimated as the temporal correlation between timeseries extracted from two ROIs. The timeseries for each ROI were obtained by extracting the first eigenvariate of all voxel-wise timeseries that overlapped with the ROI masks. Pearson correlation coefficients between the timeseries were Fischer-transformed to enhance the normality of the FC values. We used a linear mixed model to evaluate the effect of training, as described in Section II-D.6. To investigate the association between FC and the ARAT scores, we calculated Pearson correlation coefficients between the identified FC and ARAT scores at the *Pre* and *Post* sessions, as well as between the change of FC (ΔFC) and ΔARAT.

TABLE II
LINEAR MIXED MODEL RESULTS OF ARAT, FC AND WLI

	ARAT		$FC_{iM1-cM1}$		wLI_{motor}	
	β	p	β	p	β	p
Intercept	27.50	<**0.001*****	0.76	<**0.001*****	0.20	**0.01****
TIME	3.56	<**0.001*****	0.11	**0.01****	0.09	**0.01****
Age	-0.01	0.80	0.01	0.54	0.01	0.15
Gender	-0.23	0.43	-0.13	0.30	-0.01	0.92
TSS	0.15	0.06	-0.03	0.39	0.03	0.15
Stroke Type	0.06	0.87	-0.03	0.84	-0.19	**0.03***
Affected hand	0.06	0.82	0.06	0.60	0.00	0.96
pre-ARAT	0.99	<**0.001*****	0.01	0.21	0.01	0.11

Numerical variables (Age, TSS, pre-ARAT) were mean-centered. Factor and categorical variables (TIME, Gender, Stroke type, Affected hand) were represented using sum codings. Intercept denotes the average value of the metrics over both sessions. p-values were obtained from one-sample t-test of the estimates using degree-of-freedom estimated from the Satterthwaite's method. Asterisks denotes the level of statistical significance (***=p<0.001; **=p<0.01; *=p<0.05)

5) Tb-fMRI Activation Analysis: We conducted a paired t-test to examine the change in activation level during motor execution of the paretic hand between the *Pre* and *Post* sessions. The resulting t-map was corrected using Gaussian Random Field (GRF) correction (p < 0.01 voxelwise, p< 0.05 clusterwise). However, No significant cluster was identified.

To investigate the inter-hemispheric activation during motor execution, we studied the weighted Laterality Index (wLI) before and after training. First, we thresholded individual contrast maps for the IPSI condition at p < 0.001, GRF corrected at 0.05 cluster threshold. Motor-related activation was determined by overlaying individual activation maps with sensorimotor masks defined using the AAL atlas, and the included regions were listed in the Supplementary table S1. The wLI was defined as the normalized difference in activation between the ipsilesional and contralesional hemisphere, as described in Equation 2.

$$wLI = \frac{\sum_V t_I - \sum_V t_C}{\sum_V t_I + \sum_V t_C} \tag{2}$$

Here, $\sum_V t_I$ and $\sum_V t_C$ represent the sum of t-values within all significant voxels of the activation mask V at the ipsilesional and contralesional hemisphere, respectively. The wLI_{motor} measures the hemispheric dominance of the activation over the sensorimotor networks, with values ranging from -1 to 1. A value of 1 and -1 indicates exclusive activation on the ipsilesional and contralesional side, respectively.

To examine ROI-specific hemispheric balance, we extracted ROI-specific wLI using the mask obtained from the previous analysis. In particular, individual contrast maps for the IPSI conditions were summed over the masks of the identified ROI masks, respectively. Homotopic wLI (wLI_{M1}, wLI_{PMv}, wLI_{SMA}) were then obtained from Equation 2, with V being the corresponding ROI masks, respectively.

6) Statistical Analysis: We employed a linear mixed model analysis to investigate the effect of 20 sessions of EMG robot-hand training on ARAT, FC, and wLI. Specifically, we fitted the corresponding metrics in a linear mixed model, with the fixed effect variable TIME (*Pre*, *Post*). Confounding variables, including age, gender, time since stroke (TSS),

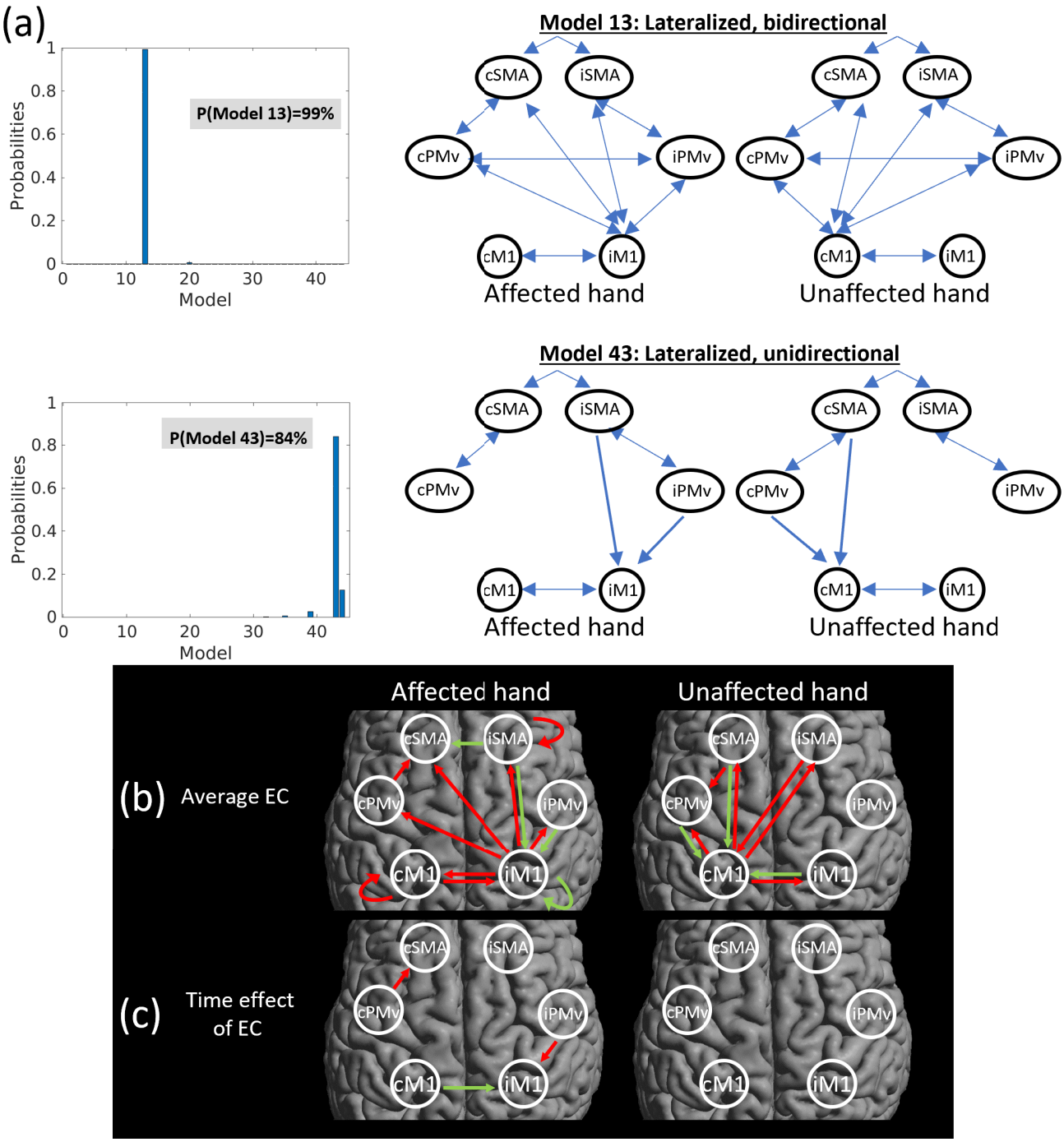

Fig. 2. (a) Models that best explain the average EC and training effect. Bayesian Model Selection over 44 candiates models were performed to determine the optimal model. Average EC and training effects were best explained by model 13 and model 14 with 99% and 84% posterior probability respectively. The right of the figure showed the corresponding architecture. A Bayesian Model Average(BMA) was subsequently performed to estimate the average EC and the time effect. (b) Average task-modulated EC during motor tasks with their affected and unaffected hand respectively. (c) Change in task-modulated EC after training. Abbreviations: EC: Effective Connectivity; M1:Primary motor cortex; PMv: Ventral Premotor Area; SMA: Supplementary Motor Area; Prefix: i-: ipsilesional; c-: contralesional.

stroke type, and affected hand, were included as covariates. Individual subjects were modeled as random effects.

The model was fitted using the restricted maximum likelihood approach (REML). The degree of freedom of the t-test for each fixed effect variable was estimated using Satterthwaite's method. We performed all statistical analyses using the lme4 and lmerTest statistical packages, which are available in R 4.2.2.

III. Result

A. Result of Training Performance and Clinical Scores

Figure 1(b) shows the training progress of all subjects, with the positive slope indicating an increase in the number of triggers with training sessions.

To compare the training effects of the different groups on ARAT scores, we conducted mixed-effect ANOVA analysis with GROUP (Control, Stimulation) and TIME (*Pre*, *Post*) as

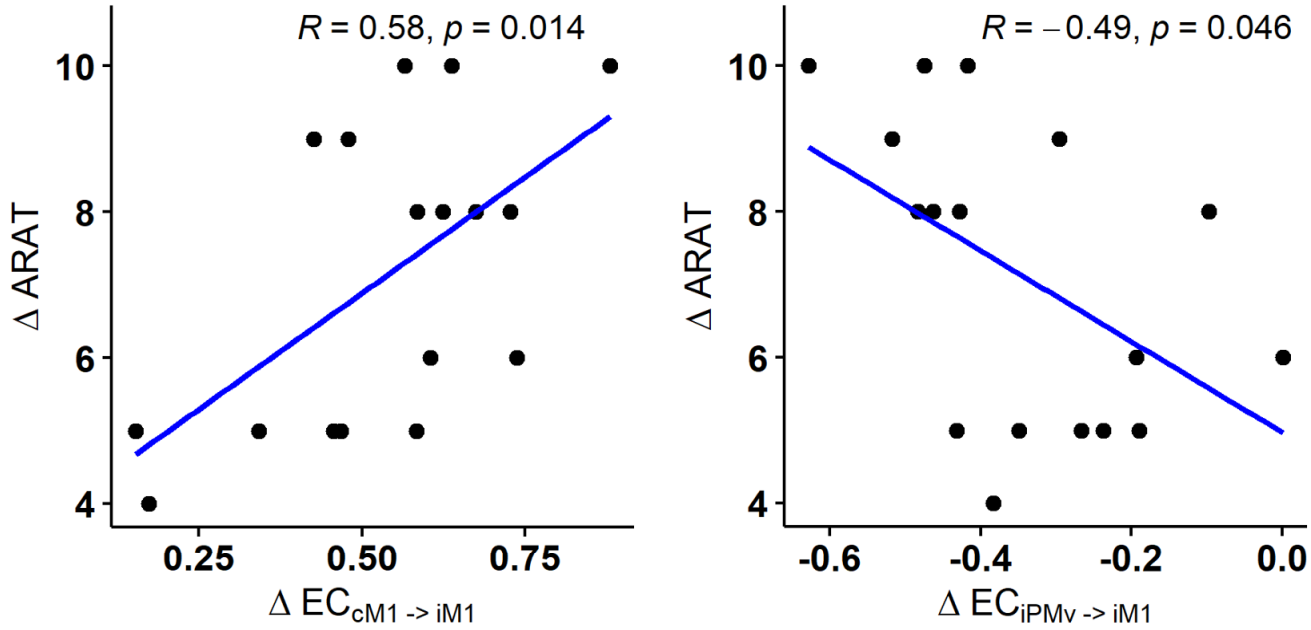

Fig. 3. Pearson correlation of effective connectivity with significant TIME effect between (a) change in effective connectivity from cM1 to iM1($\Delta EC_{cM1\rightarrow iM1}$), (b) change in effective connectivity from iPMv to iM1($\Delta EC_{iPMv\rightarrow iM1}$) and ARAT improvement(ΔARAT) after training.

fixed-effect variables. We observed a significant main effect of TIME ($F(1,34)=434.22$, $p<0.001$), but no interaction effect was observed between GROUP and TIME ($F(1,34)=4.33$, $p=0.07$). This result suggests that adjunct treatment with personalized tDCS did not perform better than sham-controlled robot-hand training in improving motor functions. Since our study focuses on investigating the treatment effect and neural correlates for EMG-robot hand training, we combined both groups to increase the overall effect size of the statistical measures. The statistical analysis is summarized in Table II, with a significant positive effect ($\beta=3.56$, $p<0.001$) observed on ARAT scores, indicating an improvement in upper extremity function after EMG robot-hand training.

B. Dynamic Causal Modeling

The average individual DCM model estimation explained 61.6% (SD 15.5%) of the fMRI data. Bayesian Model Selection over 44 reduced candidates models determined that Model 13 and Model 43 that best explains the average effective connectivity and training effect of the stroke subjects (Figure 2 (a)). We also grouped the candidate models into 4 families and the corresponding results could be found in Supplementary Results 2.6. BMA of the candidate models identified non-trivial coupling parameters obtained for the average task-modulated effective connectivity and its training effect (Figure 2(b)). All BMA parameters for A and B matrices were listed in Supplementary Table S4 and S5. Green arrows indicate facilitatory effects, and red arrows indicate inhibitory effects. The rounded arrows represent the self-connection parameters, which indicate the level of self-inhibition with a default value of 0.5Hz [49]. Reduced self-connection values indicate increased regional sensitivity that remains active for a longer period.

During motor tasks, positive and negative self-connection were observed in iM1 and cM1, respectively, during paretic hand movement. Additionally, activation of cM1 inhibits activity of iM1. These findings indicate that cM1 is more heavily involved when the paretic hand is used and exerts inhibitory influence on iM1.

After training, there was an increase in $EC_{cM1\rightarrow iM1}$ (Figure 2b), indicating a decrease in interhemispheric inhibition. Additionally, $EC_{iPMv\rightarrow iM1}$ and $EC_{cPMv\rightarrow cSMA}$ were reduced. Pearson correlation analysis identified a significant relationship between ΔARAT and $\Delta EC_{cM1\rightarrow iM1}$ ($r=0.584$, $p=0.0139$), as well as $\Delta EC_{iPMv\rightarrow iM1}$ ($r=-0.489$, $p=0.0463$) (Figure 3 a-b). However, no significant correlation was identified between $EC_{cM1\rightarrow iM1}$ and ARAT scores at *Pre* ($r=-0.174$, $p=0.504$) and *Post* ($r=-0.087$, $p=0.740$).

C. Resting-State Functional Connectivity

Significant main effect of TIME was observed in $FC_{iM1-cM1}$ and in $FC_{iSMA-cSMA}$. The average FC and time effect of FC for all pairs were demonstrated in Supplementary Results 2.7. We performed correlation analysis between them at *Pre*, *Post* and their changes respectively. We found a positive but non-significant correlation between $FC_{iM1-cM1}$ and ARAT scores at *Pre* ($r=0.402$, $p=0.110$) or *Post* ($r=0.436$, $p=0.080$), No significant change was found between $\Delta FC_{iM1-cM1}$ and ΔARAT scores ($r=0.009$, $p=0.981$). No significant correlation was found between $FC_{iM1-cM1}$ and $EC_{iM1-cM1}$ at *Pre*, *Post* and their changes.

No significant correlation was found between $FC_{iSMA-cSMA}$ with ARAT in *Pre*, *Post* and their corresponding changes

D. Task-Based fMRI Activation

Figure 4 displays the group-level activation map projected onto standard MNI space in the *Pre* and *Post* sessions. Inspection of the map reveals an overall decrease in activation

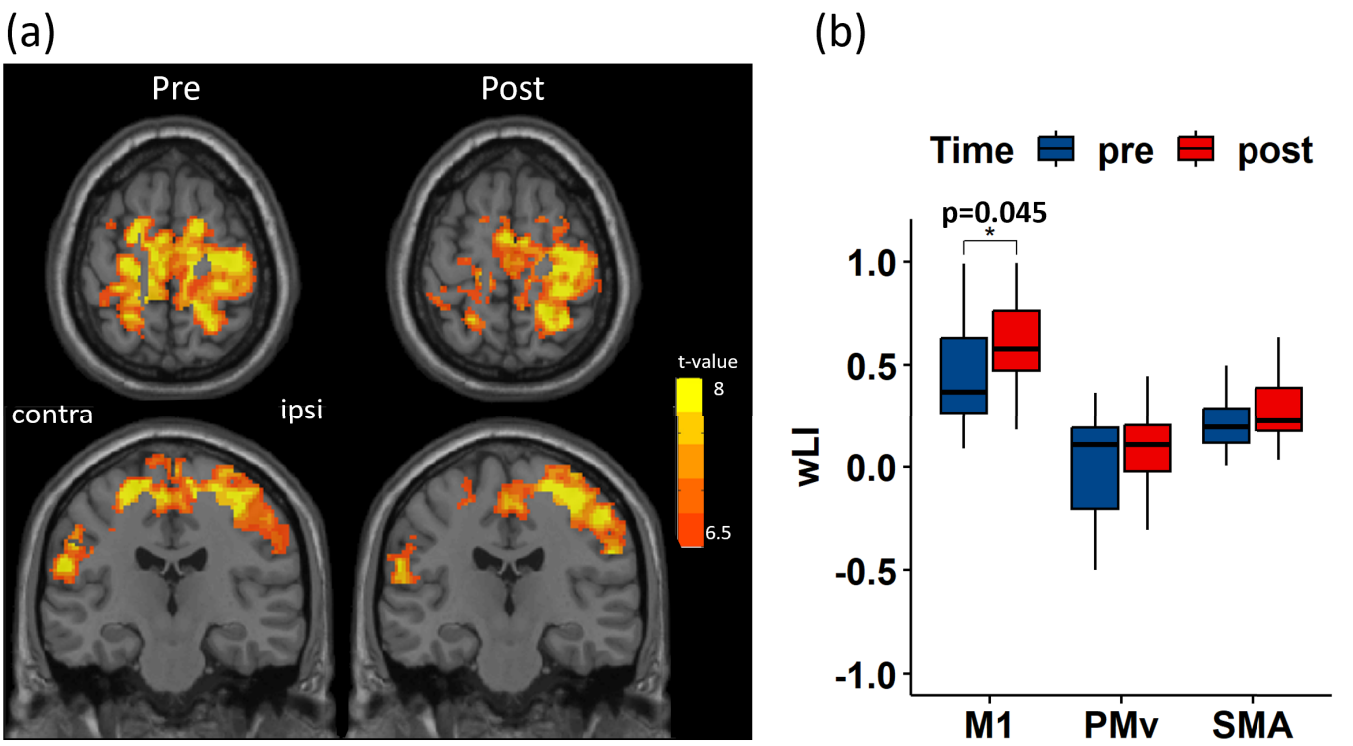

Fig. 4. Results of tb-fMRI activation analysis. (a) Group level activation map during motor execution with paretic hand in *Pre* and *Post* session respectively. Left and right side of the brain corresponds to contralesional(contra) and ipsilesional(ipsi) hemisphere respectively. (b) Boxplot showing the wLI in *Pre* and *Post* session for M1, PMv and SMA respectively. Paired t-test identified significant increase of wLI_{M1} after training.

within the contralesional hemisphere and an increase within the ipsilesional hemisphere. We found a significant positive TIME effect for wLI_{motor} (β=0.086, p=0.007) (Figure 4). For ROI-specific wLI, a significant TIME effect was only observed in wLI_{M1} (p=0.036), but not in wLI_{PMv} (p=1) or wLI_{SMA} (p=0.06).

IV. Discussion

This study aimed to investigate the neuroplastic changes in chronic stroke survivors resulting from 20 sessions of EMG-driven robot hand training. The results demonstrated a significant improvement in ARAT scores following the training. DCM analysis revealed an increase in task-modulated EC from cM1 to iM1, indicating a reduction of inter-hemispheric inhibition during motor tasks. This reduction in inter-hemispheric inhibition was positively correlated with functional improvement in the subjects. Additionally, an increase in wLI and FC between bilateral primary motor cortices indicated the restoration of inter-hemispheric balance. These results suggest that EMG-driven robot-hand training may promote the restoration of both general and task-specific inter-hemispheric balance, leading to functional recovery in the chronic phase of stroke.

According to a meta-analysis, robot-assisted upper extremity rehabilitation is more effective in improving motor functions than conventional rehabilitation interventions [5]. Among the different types of robotic devices, EMG-driven robots have demonstrated superior performance over robots that provide continuous passive motions [13]. Our findings are consistent with previous research, demonstrating the effectiveness of an EMG-driven robot in improving motor functions in chronic stroke patients. Voluntary motor intention can be decoded from EMG amplitudes of the residual muscles of the paretic hand, which triggers movement from the robot hand, providing proprioceptive feedback to the users and forming an active feedback loop [11], [50]. It is noteworthy that other intention-driven systems, particularly motor-imagery based Brain Computer Interface (BCI-MI), have been used in robot training and have shown success in post-stroke UE rehabilitation [51], [52].However, BCI-MI-driven systems are unable to facilitate descending corticospinal excitation on the target muscles [53]. In contrast, EMG-driven systems directly project motor commands from the central to peripheral system along the descending corticospinal tract, which is necessary for effective motor rehabilitation [54]. Our study confirms the rehabilitation effectiveness of the EMG-driven robotic system and further explores its neurophysiological correlates with motor recovery through fMRI analysis.

Our study revealed an increase in task-modulated effective connectivity from cM1 to iM1 after EMG-driven robot hand training, indicating a reduction in interhemispheric inhibition (IHI) from cM1 to iM1. Studies of healthy subjects have shown that IHI helps regulate motor coordination by suppressing contralateral motor activation [55]. However, individuals with chronic stroke have been found to have excessive IHI from cM1 as compared to healthy controls, with persistent suppression from cM1 to iM1 prior to movement [56], [57]. This disruptive influence of cM1 may be attributed to increased cortical compensatory activities of the contralesional hemisphere developed from the learned non-use of the paretic hand during spontaneous motor recovery [15], [58]. Our results

identified similar inhibitory effects of cM1 as reported in previous studies. Furthermore, we found a positive correlation between the reduction of IHI and the improvement of ARAT scores, indicating the role of interhemispheric interactions in the motor recovery process. To the best of our knowledge, our study is the first to demonstrate that EMG-driven robot hand interventions can modulate interhemispheric inhibition, highlighting the active role of voluntary motor intention in facilitating adaptive neural plasticity for motor recovery.

We also studied the interhemispheric reorganization by investigating the fMRI activation map during motor tasks of the paretic hand. We identified an overall increase in the wLI within the sensorimotor network after training, with the increase being significant in homotopic M1, but not in the premotor and supplementary motor area. An ipsilesional shift of activation after training indicates a decreased reliance on the unaffected hemisphere during motor tasks with the paretic hand. Low laterality characterized by strong bilateral activation of the motor area has been shown to contribute significantly to the UE motor deficits in chronic stroke [42], [58]. A series of TMS studies showed that the reduction of fMRI laterality was associated with unbalanced transcallosal inhibition between bilateral primary motor cortex during unilateral movements [59], [60], and the increase in fMRI laterality indicates an increase in ipsilesional corticomotor maps [59].An increased in ipsilesional activation and laterality during unimanual task after robot-assisted training had been reported in multiple studies [21], [51], [61]. Our result is the first to report a simultaneous increase in fMRI laterality and a reduction in IHI, providing additional insights regarding the nature of the interhemispheric balance. Particularly, reliance on non-paretic forelimb and compensatory movements of proximal limb and trunk increased the recruitment of cM1 [15], [62]. Repetitive training of EMG-driven robot hand have shown to improve patient's FMA-UE scores, and reduce compensation from proximal joints during grasping [23]. Combining the results with our findings suggest that EMG-driven robot hand facilitates independent motor control in which a gradual less reliance on cM1 was developed.The supressed cM1 activity exerted less inhibitory pressure to the iM1 activity, shaping the cortical activation towards normalized hemispheric balance.

In addition to task-based EC, rs-MRI has emerged as a valuable tool for investigating task-independent interactions between brain regions following stroke. Our findings revealed a significant increase in inter-M1 FC following training, indicating a restoration of the inter-hemispheric balance of resting-state brain activity. Several fMRI studies have reported significant reductions in inter-M1 functional connectivity during the acute and sub-acute phases of stroke, which can be attributed to the disruption of white matter tracts in the transcallosal motor fibers [63], [64]. It has been observed that individuals with good functional recovery have larger inter-M1 FC values, which resemble those of healthy controls, while individuals with poor recovery demonstrate persistently low inter-M1 FC values [40]. Our results identified a positive, marginally-significant correlation between inter-M1 FC and pre- and post-ARAT scores, which validates its prognostic value on hand motor functions. Interestingly, while we did not find any correlations between changes in inter-M1 FC and improvements in ARAT, we did identify relationships between the changes in inter-M1 EC and changes in ARAT. A TMS study conducted by Xu et al. demonstrated that the emergence of IHI from acute to chronic phase, rather than the magnitude of IHI, predicts poor recovery of finger individuation in chronic stroke [57]. Our findings suggest that the training-induced improvement of ARAT might be related to restoration the emerged maladaptive IHI back to a normal level. Combining these results, we discovered that interhemispheric FC and EC provide distinct information. Task-independent FC may reflect an individual's motor performance, while EC appears to indicate the state of motor recovery.

In addition to the inter-hemispheric change within M1, the premotor areas including PMv and SMA are also dynamically reorganized after motor training. Our results show a reduction in the facilitatory coupling from the iPMv to iM1, which is positively correlated with improvements in motor function as measured by the ARAT. PMv plays a crucial role in object manipulation and the integration of multisensory information, as demonstrated in previous studies [65], [66]. The observed reduction in iPMv facilitation seems counter-intuitive, as it contradicts the expected supportive role of iPMv-iM1 interactions in motor recovery as illustrated in previous DCM studies [32], [41]. A previous EEG study reported a similar negative association between iPMv-iM1 coupling and motor recovery [67]. A possible explanation for our observation is that robot-hand training facilitates independent finger control during object grasping which leads to a reduction in iPMv facilitation. Compensatory strategies are frequently observed in stroke during grasping, in which individuals over-adjusted their proximal joint in the reach, and open hand excessively to grasp with excessive force [15]. EMG-driven robot hand practised voluntary finger grasping and opening, which was shown to improve individual's finger dexterity measured by Finger Individuation Index [13], reduce finger spasticity and reliance on proximal muscles [23]. Paired-pulse TMS studies have shown that PMv-M1 facilitation effects are specific to the active muscles [68]. Furthermore, PMv was also shown to inhibit non-target muscles for coordination and production of complex hand postures in animal studies [69], [70]. Our results suggest a possibility that the improvement of independent finger control, partially represented by ARAT score changes, reduced the activation of non-target muscles during object grasping. A reduced iPMv-iM1 facilitation might therefore imply a more efficient information flow in execution of finger movements. Additionally, we observed an increased inhibitory effect from the cPMv to cSMA after training. Previous studies have reported that the contralesional premotor cortex supports the residual motor function in stroke patients [71]. Longitudinal fMRI studies have identified decreased activation of cPMv and cSMA during the process of motor recovery [72]. However, some studies have also suggested the supportive role of cSMA in motor inhibition control and bimanual coordination [73], [74]. Our results identified an average inhibitory effect from cSMA to the contralateral M1 (cM1) during paretic

hand movements, suggesting that cSMA was involved in down-regulating cM1 excitability during motor tasks with the affected hand. A previous study comparing motor execution and imagery reported higher effective connectivity during motor execution, suggesting the presence of PMv-SMA interactions in generating actual motor outputs [75]. The study hypothesized that PMv reacts to external stimuli to generate action commands relayed to the SMA for movement initiation. Applying this hypothesis to our findings, the observed reduction in cPMv-cSMA coupling may indicate less interference from the non-paretic hand and greater focus on paretic hand movements.

In this study, we combined the stimulation and control groups to assess the overall training effect of EMG-robot hand training on cortical reorganization. While this approach allowed us to increase the effect size of neurophysiological factors by pooling data from both groups, We are aware that a marginally significant interaction effect was observed between stimulation group and training effect, indicating a potential beneficial effect of personalized tDCS. Further studies with larger sample sizes and the use of multiple neuroimaging and clinical assessment modalities are needed to uncover the full effect of training augmented with tDCS. Consideration of group-specific training effect in future studies to better understand the mechanisms underlying the training effect of EMG-robot hand training and develop better rehabilitation strategies incorporating with neuromodulation technology.

REFERENCES

[1] E. S. Lawrence et al., "Estimates of the prevalence of acute stroke impairments and disability in a multiethnic population," *Stroke*, vol. 32, no. 6, pp. 1279–1284, Jun. 2001.

[2] G. Kwakkel, B. J. Kollen, J. van der Grond, and A. J. H. Prevo, "Probability of regaining dexterity in the flaccid upper limb," *Stroke*, vol. 34, no. 9, pp. 2181–2186, Sep. 2003.

[3] X. Xue et al., "Global trends and hotspots in research on rehabilitation robots: A bibliometric analysis from 2010 to 2020," *Frontiers Public Health*, vol. 9, Jan. 2022, Art. no. 806723.

[4] P. Sanchetee, "Current trends in stroke rehabilitation," in *Ischemic Stroke*, P. Sanchetee, Ed. London, U.K.: IntechOpen, 2021.

[5] J. Wu, H. Cheng, J. Zhang, S. Yang, and S. Cai, "Robot-assisted therapy for upper extremity motor impairment after stroke: A systematic review and meta-analysis," *Phys. Therapy*, vol. 101, no. 4, Apr. 2021, Art. no. pzab010.

[6] L. Zhang, G. Jia, J. Ma, S. Wang, and L. Cheng, "Short and long-term effects of robot-assisted therapy on upper limb motor function and activity of daily living in patients post-stroke: A meta-analysis of randomized controlled trials," *J. NeuroEng. Rehabil.*, vol. 19, no. 1, p. 76, Dec. 2022.

[7] J. M. Veerbeek et al., "Effects of robot-assisted therapy for the upper limb after stroke: A systematic review and meta-analysis," *Neurorehabil. Neural Repair*, vol. 31, no. 2, pp. 107–121, 2017.

[8] C. Liu, J. Lu, H. Yang, and K. Guo, "Current state of robotics in hand rehabilitation after stroke: A systematic review," *Appl. Sci.*, vol. 12, no. 9, p. 4540, Apr. 2022.

[9] S. Dehem et al., "Effectiveness of upper-limb robotic-assisted therapy in the early rehabilitation phase after stroke: A single-blind, randomised, controlled trial," *Ann. Phys. Rehabil. Med.*, vol. 62, no. 5, pp. 313–320, Sep. 2019.

[10] Y. Huang, W. P. Lai, Q. Qian, X. Hu, E. W. C. Tam, and Y. Zheng, "Translation of robot-assisted rehabilitation to clinical service: A comparison of the rehabilitation effectiveness of EMG-driven robot hand assisted upper limb training in practical clinical service and in clinical trial with laboratory configuration for chronic stroke," *Biomed. Eng. OnLine*, vol. 17, no. 1, p. 91, Dec. 2018.

[11] R. Song, K.-Y. Tong, X. Hu, and L. Li, "Assistive control system using continuous myoelectric signal in robot-aided arm training for patients after stroke," *IEEE Trans. Neural Syst. Rehabil. Eng.*, vol. 16, no. 4, pp. 371–379, Aug. 2008.

[12] X. L. Hu, K.-Y. Tong, R. Song, X. J. Zheng, and W. W. F. Leung, "A comparison between electromyography-driven robot and passive motion device on wrist rehabilitation for chronic stroke," *Neurorehabilitation Neural Repair*, vol. 23, no. 8, pp. 837–846, Oct. 2009.

[13] E. A. Susanto, R. K. Tong, C. Ockenfeld, and N. S. Ho, "Efficacy of robot-assisted fingers training in chronic stroke survivors: A pilot randomized-controlled trial," *J. NeuroEng. Rehabil.*, vol. 12, no. 1, p. 42, Dec. 2015.

[14] Z. Warraich and J. A. Kleim, "Neural plasticity: The biological substrate for neurorehabilitation," *PM&R*, vol. 2, no. 12S, pp. S208–S219, Dec. 2010.

[15] T. A. Jones, "Motor compensation and its effects on neural reorganization after stroke," *Nature Rev. Neurosci.*, vol. 18, no. 5, pp. 267–280, May 2017.

[16] N. Takeuchi and S.-I. Izumi, "Maladaptive plasticity for motor recovery after stroke: Mechanisms and approaches," *Neural Plasticity*, vol. 2012, pp. 1–9, Jun. 2012.

[17] L. J. Boddington and J. N. J. Reynolds, "Targeting interhemispheric inhibition with neuromodulation to enhance stroke rehabilitation," *Brain Stimulation*, vol. 10, no. 2, pp. 214–222, Mar. 2017.

[18] J. Liepert, F. Hamzei, and C. Weiller, "Motor cortex disinhibition of the unaffected hemisphere after acute stroke," *Muscle Nerve*, vol. 23, no. 11, pp. 1761–1763, 2000.

[19] S. Schwerin, J. P. A. Dewald, M. Haztl, S. Jovanovich, M. Nickeas, and C. MacKinnon, "Ipsilateral versus contralateral cortical motor projections to a shoulder adductor in chronic hemiparetic stroke: Implications for the expression of arm synergies," *Exp. Brain Res.*, vol. 185, no. 3, pp. 509–519, Mar. 2008.

[20] M. Maier, B. R. Ballester, and P. F. M. J. Verschure, "Principles of neurorehabilitation after stroke based on motor learning and brain plasticity mechanisms," *Frontiers Syst. Neurosci.*, vol. 13, p. 74, Dec. 2019.

[21] L. Bonanno et al., "Neural plasticity changes induced by motor robotic rehabilitation in stroke patients: The contribution of functional neuroimaging," *Bioengineering*, vol. 10, no. 8, p. 990, Aug. 2023.

[22] K. B. Wilkins, M. Owen, C. Ingo, C. Carmona, J. P. A. Dewald, and J. Yao, "Neural plasticity in moderate to severe chronic stroke following a device-assisted task-specific arm/hand intervention," *Frontiers Neurol.*, vol. 8, p. 284, Jun. 2017.

[23] Z. Guo et al., "Corticomuscular integrated representation of voluntary motor effort in robotic control for wrist-hand rehabilitation after stroke," *J. Neural Eng.*, vol. 19, no. 2, Mar. 2022, Art. no. 026004.

[24] N. Singh, M. Saini, N. Kumar, M. V. P. Srivastava, and A. Mehndiratta, "Evidence of neuroplasticity with robotic hand exoskeleton for post-stroke rehabilitation: A randomized controlled trial," *J. NeuroEng. Rehabil.*, vol. 18, no. 1, p. 76, May 2021.

[25] C. Grefkes and G. R. Fink, "Connectivity-based approaches in stroke and recovery of function," *Lancet Neurol.*, vol. 13, no. 2, pp. 206–216, Feb. 2014.

[26] E. A. Fridman, "Reorganization of the human ipsilesional premotor cortex after stroke," *Brain*, vol. 127, no. 4, pp. 747–758, Jan. 2004.

[27] P. Nachev, H. Wydell, K. O'Neill, M. Husain, and C. Kennard, "The role of the pre-supplementary motor area in the control of action," *NeuroImage*, vol. 36, pp. T155–T163, Jan. 2007.

[28] F. Hoffstaedter, C. Grefkes, K. Zilles, and S. B. Eickhoff, "The 'what' and 'When' of self-initiated movements," *Cerebral Cortex*, vol. 23, no. 3, pp. 520–530, Mar. 2013.

[29] P. A. Chouinard, "Different roles of PMv and PMd during object lifting," *J. Neurosci.*, vol. 26, no. 24, pp. 6397–6398, Jun. 2006.

[30] N. Doganci, G. R. Iannotti, and R. Ptak, "Task-based functional connectivity identifies two segregated networks underlying intentional action," *NeuroImage*, vol. 268, Mar. 2023, Art. no. 119866.

[31] C. Grefkes et al., "Cortical connectivity after subcortical stroke assessed with functional magnetic resonance imaging," *Ann. Neurol.*, vol. 63, no. 2, pp. 236–246, Feb. 2008.

[32] A. K. Rehme, S. B. Eickhoff, L. E. Wang, G. R. Fink, and C. Grefkes, "Dynamic causal modeling of cortical activity from the acute to the chronic stage after stroke," *NeuroImage*, vol. 55, no. 3, pp. 1147–1158, Apr. 2011.

[33] C. Grefkes, D. A. Nowak, L. E. Wang, M. Dafotakis, S. B. Eickhoff, and G. R. Fink, "Modulating cortical connectivity in stroke patients by rTMS assessed with fMRI and dynamic causal modeling," *NeuroImage*, vol. 50, no. 1, pp. 233–242, Mar. 2010.

[34] P. Zeidman et al., "A guide to group effective connectivity analysis—Part 2: Second level analysis with PEB," *NeuroImage*, vol. 200, pp. 12–25, Oct. 2019.

[35] M. D. Fox and M. E. Raichle, "Spontaneous fluctuations in brain activity observed with functional magnetic resonance imaging," *Nature Rev. Neurosci.*, vol. 8, no. 9, pp. 700–711, Sep. 2007.

[36] S. Ogawa, T. M. Lee, A. R. Kay, and D. W. Tank, "Brain magnetic resonance imaging with contrast dependent on blood oxygenation," *Proc. Nat. Acad. Sci. USA*, vol. 87, no. 24, pp. 9868–9872, Dec. 1990.

[37] L. Wang et al., "Dynamic functional reorganization of the motor execution network after stroke," *Brain*, vol. 133, no. 4, pp. 1224–1238, Apr. 2010.

[38] C.-H. Park et al., "Longitudinal changes of resting-state functional connectivity during motor recovery after stroke," *Stroke*, vol. 42, no. 5, pp. 1357–1362, May 2011.

[39] A. R. Carter et al., "Resting interhemispheric functional magnetic resonance imaging connectivity predicts performance after stroke," *Ann. Neurol.*, vol. 67, no. 3, pp. 365–375, Mar. 2010.

[40] Y.-S. Min et al., "Interhemispheric functional connectivity in the primary motor cortex assessed by resting-state functional magnetic resonance imaging aids long-term recovery prediction among subacute stroke patients with severe hand weakness," *J. Clin. Med.*, vol. 9, no. 4, p. 975, Apr. 2020.

[41] T. Paul et al., "Early motor network connectivity after stroke: An interplay of general reorganization and state-specific compensation," *Hum. Brain Mapping*, vol. 42, no. 16, pp. 5230–5243, Nov. 2021.

[42] S. Zhou et al., "Pathway-specific cortico-muscular coherence in proximal-to-distal compensation during fine motor control of finger extension after stroke," *J. Neural Eng.*, vol. 18, no. 5, Sep. 2021, Art. no. 056034.

[43] X. L. Hu, K. Y. Tong, X. J. Wei, W. Rong, E. A. Susanto, and S. K. Ho, "The effects of post-stroke upper-limb training with an electromyography (EMG)-driven hand robot," *J. Electromyogr. Kinesiol.*, vol. 23, no. 5, pp. 1065–1074, Oct. 2013.

[44] C.-G. Yan, X.-D. Wang, X.-N. Zuo, and Y.-F. Zang, "DPABI: Data processing & analysis for (resting-state) brain imaging," *Neuroinformatics*, vol. 14, no. 3, pp. 339–351, Jul. 2016.

[45] J. Ashburner, "A fast diffeomorphic image registration algorithm," *NeuroImage*, vol. 38, no. 1, pp. 95–113, Oct. 2007.

[46] L. Giulia et al., "The impact of neurofeedback on effective connectivity networks in chronic stroke patients: An exploratory study," *J. Neural Eng.*, vol. 18, no. 5, Oct. 2021, Art. no. 056052.

[47] E. T. Rolls, C.-C. Huang, C.-P. Lin, J. Feng, and M. Joliot, "Automated anatomical labelling atlas 3," *NeuroImage*, vol. 206, Feb. 2020, Art. no. 116189.

[48] K. J. Friston et al., "Bayesian model reduction and empirical Bayes for group (DCM) studies," *NeuroImage*, vol. 128, pp. 413–431, Mar. 2016.

[49] P. Zeidman et al., "A guide to group effective connectivity analysis—Part 1: First level analysis with DCM for fMRI," *NeuroImage*, vol. 200, pp. 174–190, Oct. 2019.

[50] N. S. K. Ho et al., "An EMG-driven exoskeleton hand robotic training device on chronic stroke subjects: Task training system for stroke rehabilitation," in *Proc. IEEE Int. Conf. Rehabil. Robot.*, Jun. 2011, pp. 1–5.

[51] K. Yuan, X. Wang, C. Chen, C. C. Lau, W. C. Chu, and R. K. Tong, "Interhemispheric functional reorganization and its structural base after BCI-guided upper-limb training in chronic stroke," *IEEE Trans. Neural Syst. Rehabil. Eng.*, vol. 28, no. 11, pp. 2525–2536, Nov. 2020.

[52] K. K. Ang et al., "A randomized controlled trial of EEG-based motor imagery brain-computer interface robotic rehabilitation for stroke," *Clin. EEG Neurosci.*, vol. 46, no. 4, pp. 310–320, Oct. 2015.

[53] Z. Bai, K. N. K. Fong, J. J. Zhang, J. Chan, and K. H. Ting, "Immediate and long-term effects of BCI-based rehabilitation of the upper extremity after stroke: A systematic review and meta-analysis," *J. NeuroEng. Rehabil.*, vol. 17, no. 1, p. 57, Dec. 2020.

[54] C. L. Witham, C. N. Riddle, M. R. Baker, and S. N. Baker, "Contributions of descending and ascending pathways to corticomuscular coherence in humans," *J. Physiol.*, vol. 589, no. 15, pp. 3789–3800, Aug. 2011.

[55] B. W. Fling and R. D. Seidler, "Task-dependent effects of interhemispheric inhibition on motor control," *Behavioural Brain Res.*, vol. 226, no. 1, pp. 211–217, Jan. 2012.

[56] A. N. H. Gerges, B. Hordacre, F. D. Pietro, G. L. Moseley, and C. Berryman, "Do adults with stroke have altered interhemispheric inhibition? A systematic review with meta-analysis," *J. Stroke Cerebrovascular Diseases*, vol. 31, no. 7, Jul. 2022, Art. no. 106494.

[57] J. Xu et al., "Rethinking interhemispheric imbalance as a target for stroke neurorehabilitation," *Ann. Neurol.*, vol. 85, no. 4, pp. 502–513, Apr. 2019.

[58] J. G. McPherson, A. Chen, M. D. Ellis, J. Yao, C. J. Heckman, and J. P. A. Dewald, "Progressive recruitment of contralesional cortico-reticulospinal pathways drives motor impairment post stroke," *J. Physiol.*, vol. 596, no. 7, pp. 1211–1225, Apr. 2018.

[59] D. A. Cunningham et al., "Assessment of inter-hemispheric imbalance using imaging and noninvasive brain stimulation in patients with chronic stroke," *Arch. Phys. Med. Rehabil.*, vol. 96, no. 4, pp. S94–S103, Apr. 2015.

[60] F. Giovannelli et al., "Modulation of interhemispheric inhibition by volitional motor activity: An ipsilateral silent period study," *J. Physiol.*, vol. 587, no. 22, pp. 5393–5410, Nov. 2009.

[61] C. Chen, K. Yuan, X. Wang, A. Khan, W. C.-W. Chu, and R. K.-Y. Tong, "Neural correlates of motor recovery after robot-assisted training in chronic stroke: A multimodal neuroimaging study," *Neural Plasticity*, vol. 2021, pp. 1–12, Jun. 2021.

[62] L. R. Montgomery, W. J. Herbert, and J. A. Buford, "Recruitment of ipsilateral and contralateral upper limb muscles following stimulation of the cortical motor areas in the monkey," *Exp. Brain Res.*, vol. 230, no. 2, pp. 153–164, Oct. 2013.

[63] J. L. Chen and G. Schlaug, "Resting state interhemispheric motor connectivity and white matter integrity correlate with motor impairment in chronic stroke," *Frontiers Neurol.*, vol. 4, p. 178, Nov. 2013.

[64] J. Liu, C. Wang, J. Cheng, P. Miao, and Z. Li, "Dynamic relationship between interhemispheric functional connectivity and corticospinal tract changing pattern after subcortical stroke," *Frontiers Aging Neurosci.*, vol. 14, May 2022, Art. no. 870718.

[65] A. T. Reader and N. P. Holmes, "The left ventral premotor cortex is involved in hand shaping for intransitive gestures: Evidence from a two-person imitation experiment," *Roy. Soc. Open Sci.*, vol. 5, no. 10, Oct. 2018, Art. no. 181356.

[66] D. Zeller, C. Gross, A. Bartsch, H. Johansen-Berg, and J. Classen, "Ventral premotor cortex may be required for dynamic changes in the feeling of limb ownership: A lesion study," *J. Neurosci.*, vol. 31, no. 13, pp. 4852–4857, Mar. 2011.

[67] J. M. Cassidy, A. Wodeyar, R. Srinivasan, and S. C. Cramer, "Coherent neural oscillations inform early stroke motor recovery," *Hum. Brain Mapping*, vol. 42, no. 17, pp. 5636–5647, Dec. 2021.

[68] M. Davare, K. Montague, E. Olivier, J. C. Rothwell, and R. N. Lemon, "Ventral premotor to primary motor cortical interactions during object-driven grasp in humans," *Cortex*, vol. 45, no. 9, pp. 1050–1057, Oct. 2009.

[69] G. Prabhu et al., "Modulation of primary motor cortex outputs from ventral premotor cortex during visually guided grasp in the macaque monkey," *J. Physiol.*, vol. 587, no. 5, pp. 1057–1069, Mar. 2009.

[70] S. Quessy, S. L. Côté, A. Hamadjida, J. Deffeyes, and N. Dancause, "Modulatory effects of the ipsi and contralateral ventral premotor cortex (PMv) on the primary motor cortex (M1) outputs to intrinsic hand and forearm muscles inCebus apella," *Cerebral Cortex*, vol. 26, no. 10, pp. 3905–3920, Oct. 2016.

[71] S. Bestmann et al., "The role of contralesional dorsal premotor cortex after stroke as studied with concurrent TMS-fMRI," *J. Neurosci.*, vol. 30, no. 36, pp. 11926–11937, Sep. 2010.

[72] N. S. Ward, "Neural correlates of motor recovery after stroke: A longitudinal fMRI study," *Brain*, vol. 126, no. 11, pp. 2476–2496, Nov. 2003.

[73] C. Wardak, "The role of the supplementary motor area in inhibitory control in monkeys and humans," *J. Neurosci.*, vol. 31, no. 14, pp. 5181–5183, Apr. 2011.

[74] N. Sadato, Y. Yonekura, A. Waki, H. Yamada, and Y. Ishii, "Role of the supplementary motor area and the right premotor cortex in the coordination of bimanual finger movements," *J. Neurosci.*, vol. 17, no. 24, pp. 9667–9674, Dec. 1997.

[75] Y. K. Kim, E. Park, A. Lee, C.-H. Im, and Y.-H. Kim, "Changes in network connectivity during motor imagery and execution," *PLoS ONE*, vol. 13, no. 1, Jan. 2018, Art. no. e0190715.